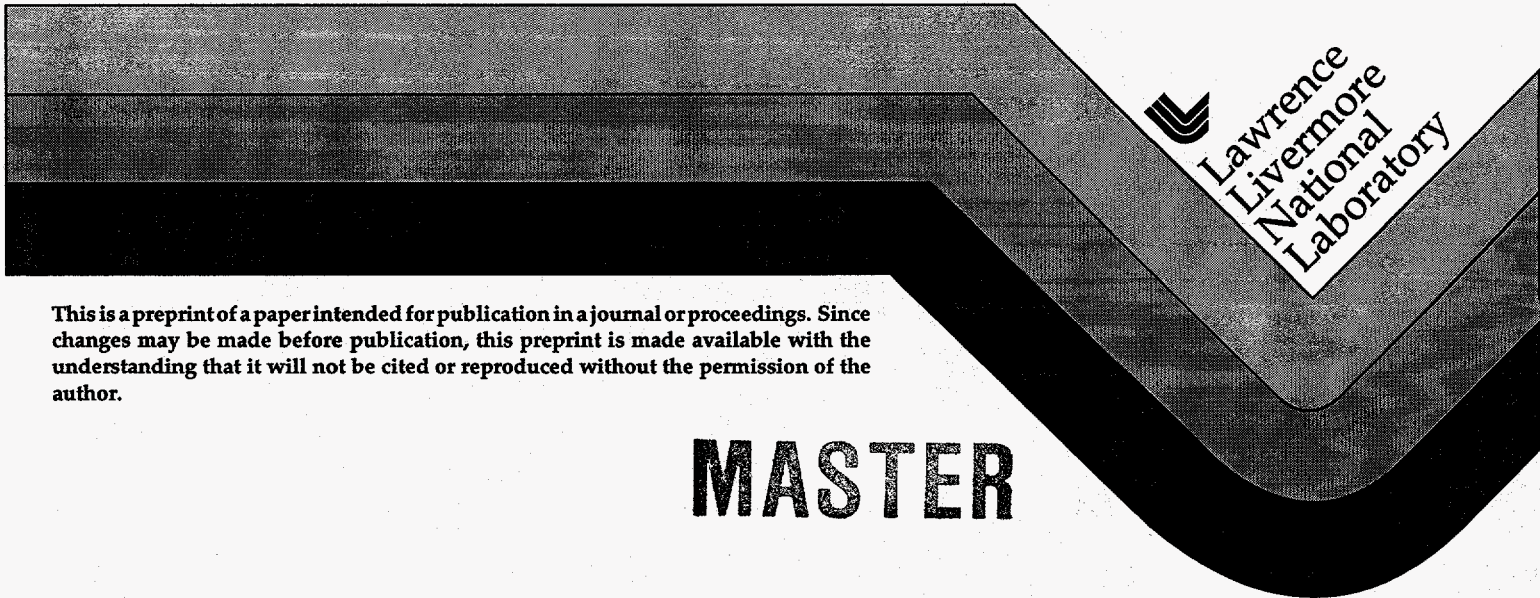CONF-961005--11

RECEIVED

DEC 0 9 1996

OSTI

Progress on the Physics of Ignition for Radiation Driven Inertial Confinement Fusion (ICF) Targets

J. D. Lindl
M. M. Marinak

September 1996

Lawrence
Livermore
National
Laboratory

MASTER

MASTER

DISCLAIMER

DISCLAIMER

Portions of this document may be illegible in electronic image products. Images are produced from the best available original document.

PROGRESS ON THE PHYSICS OF IGNITION FOR RADIATION DRIVEN INERTIAL CONFINEMENT FUSION (ICF) TARGETS

J. D. LINDL and M. M. MARINAK
Lawrence Livermore National Laboratory, Livermore, California, USA

Abstract

PROGRESS ON THE PHYSICS OF IGNITION FOR RADIATION DRIVEN INERTIAL CONFINEMENT FUSION (ICF) TARGETS.

Extensive modeling of proposed National Ignition Facility (NIF) ignition targets has resulted in a variety of targets using different materials in the fuel shell, using driving temperatures which range from 250-300 eV, and requiring energies which range from less than 1 MJ up to the full 1.8 MJ design capability of the NIF. Recent experiments on Nova have shown that hohlraum walls composed of a mixture of high-z materials could result in targets which require about 20% less energy.

Nova experiments are being used to quantify the benefits of beam smoothing in reducing stimulated scattering processes and laser beam filamentation for proposed gas-filled hohlraum targets on the NIF. Use of Smoothing by Spectral Dispersion (SSD) with 2-3 Å of bandwidth results in <4-5% of Stimulated Raman Scattering (SRS) and less than about 1% Stimulated Brillouin Scattering (SBS) for intensities less than about $2x10^{15}$ W/cm^2 for this type of hohlraum. The symmetry in Nova gas-filled hohlraums is affected by the gas fill. A large body of evidence now exists which indicates that this effect is due to laser beam filamentation which can be largely controlled by beam smoothing.

We present here the first 3-D simulations of hydrodynamic instability for the NIF point design capsule. These simulations, with the HYDRA radiation hydrodynamics code, indicate that spikes can penetrate up to 10 μm into the 30 μm radius hot spot before ignition is quenched.

Using capsules whose surface is modified by laser ablation, Nova experiments have been used to quantify the degradation of implosions subject to near NIF levels of hydrodynamic instability.

The ignition threshold for radiation driven ICF targets, as indicated in Fig. 1, is governed by the limitations imposed by laser-plasma interactions, which affect the peak driving flux and symmetry of x rays in hohlraums, and by the growth of hydrodynamic instabilities in the imploding shell containing the fusion fuel, which sets a minimum on the required driving pressure
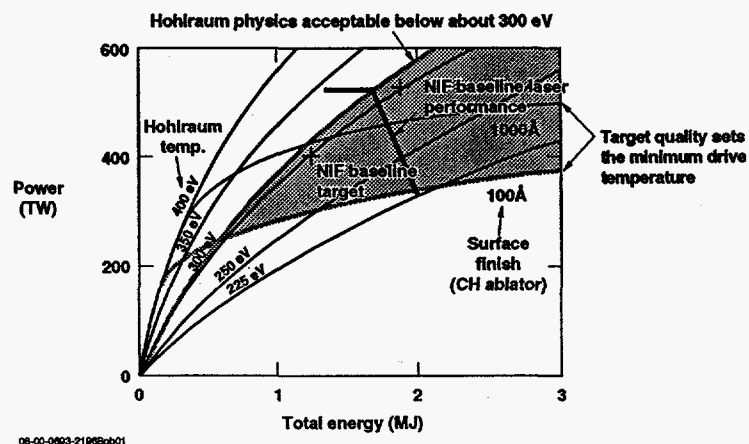

Fig. 1   Plasma physics issues constrain the achievable hohlraum temperatures and hydrodynamic instabilities establish the minimum required temperatures for ignition. Above about 0.6-1.0 MJ, depending on target surface finish, there is a region in laser power/energy space consistent with ignition

(or radiation flux)[1]. Laser/plasma parametric instabilities limit radiation temperatures in long pulse hohlraums suitable for ignition, to about 300 eV. Hydrodynamic instabilities, which enforce a minimum drive pressure, place a minimum temperature requirement of about 250 eV for the NIF. Hence, the NIF has about a factor of 2 margin in both power and energy above the ignition threshold.

Increasingly detailed LASNEX[2] computer calculations[3,4] carried out over the past several years have identified a wide variety of potential target designs which can achieve ignition. Targets have been evaluated which achieve ignition over a range of energies from 0.9 MJ to the full 1.8 MJ of the NIF and from 250 eV to 300 eV. In addition, a variety of materials including various plastics, beryllium, and B_4C can be used as ablators on the fuel capsule.

Figure 2 shows a schematic of the target design, the PT design, which has had the most detailed analysis. It uses a plastic ablator doped with Ge for the fuel capsule which also contains a cryogenic layer of DT. The hohlraum has Au walls and is filled with a mixture of He/H gas. Two rings of beams, with independent pulse shape, from each side are located to provide symmetry. Typical LASNEX calculations include the laser propagation and deposition, x-ray production and transport, material evolution in the hohlraum and the capsule implosion in a single integrated calculation. The numerical grid and the laser rays from a calculation of the PT design at peak power is shown in Fig. 3. The performance of the PT design at various sizes, corresponding to the laser energies indicated, is shown in Fig. 4. Asymmetry modeling from the integrated LASNEX calculations is used to determine how good the symmetry must be, and provides specifications on the NIF. The principal sources of capsule nonuniformity are capsule perturbations from the ablator and cryogenic fuel and nonuniformities in the radiation flux produced in the hohlraum. From the simulations we find that these various sources add approximately in quadrature so we require:

$$\left(\frac{\text{Cryo layer Nonuniformity}}{\text{Max Tolerable}}\right)^2 + \left(\frac{\text{Ablator Nonuniformity}}{\text{Max Tolerable}}\right)^2 + \left(\frac{\text{Symmetry Nonuniformity}}{\text{Max Tolerable}}\right)^2 < 1$$
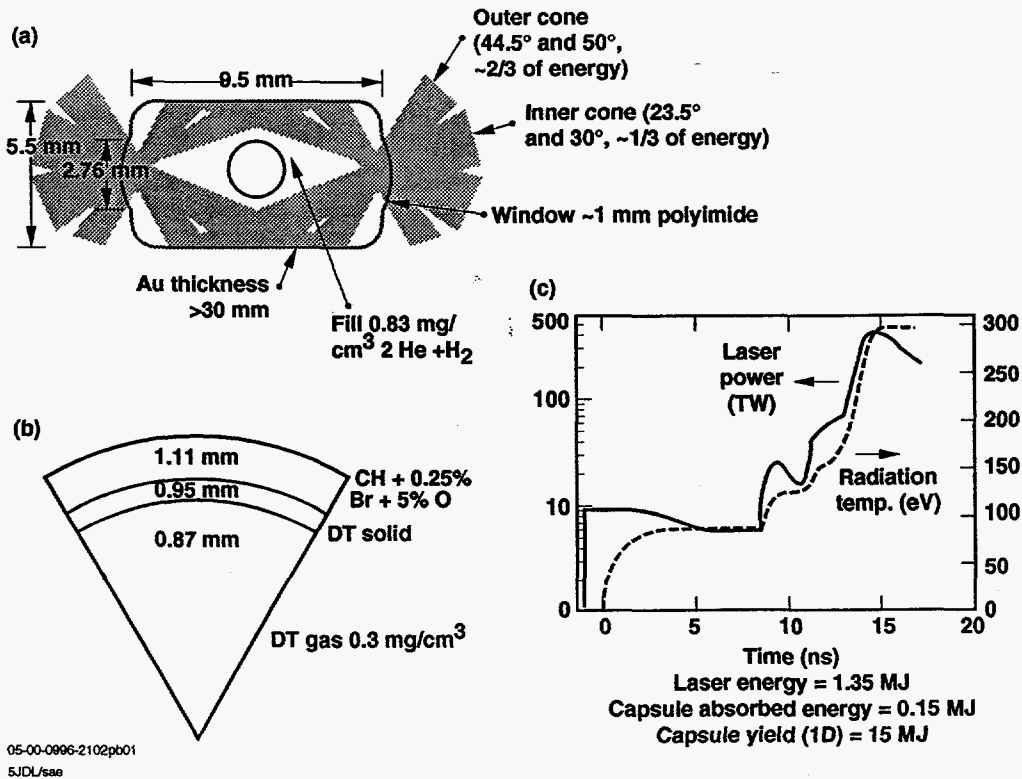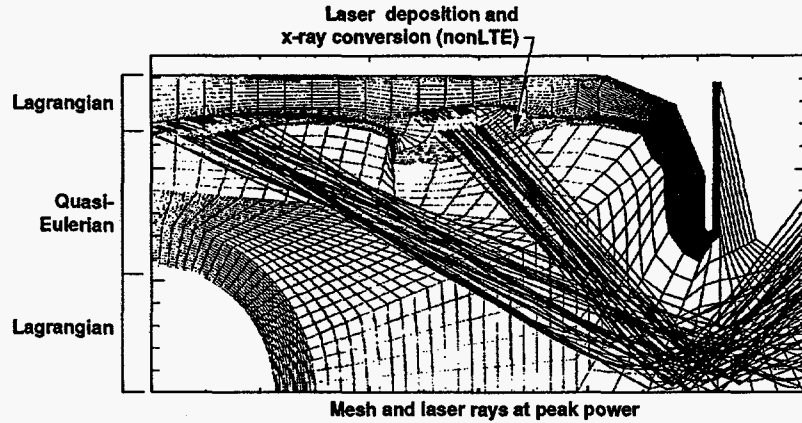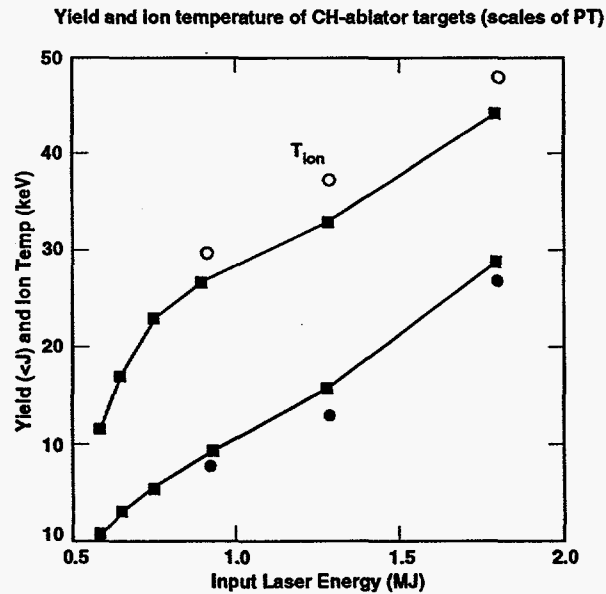

05-00-0996-2102pb01
5JDL/sae

Fig. 2   Most of the LASNEX integrated modeling and detailed analysis of Rayleigh-Taylor instability has concentrated on a target, called the PT, which absorbs about 1.3 MJ of 0.35 μm laser light.

2

**Laser deposition and
x-ray conversion (nonLTE)**

Mesh and laser rays at peak power

05-00-0996-2103pb01
SJDL/mom

Fig. 3 Integrated LASNEX simulations include in one simulation, all the physics except small-scale hydrodynamic instability and laser-plasma instability growth. Shown is a numerical grid at the peak of the laser pulse. The calculation has a plane of mirror symmetry about the left vertical axis and an axis of rotation about the lower horizontal axis.

Yield and Ion temperature of CH-ablator targets (scales of PT)

05-00-0996-2104
SJDL/sae

Fig. 4 In integrated calculations, the ignition threshold is less than 1 MJ for scales of the PT. Circles are from 2D LASNEX integrated calculations. The lines are from 1D calculations.

In order for the effects of long wavelength flux nonuniformity from the hohlraum to be about comparable to the shorter spatial scale perturbations from the ablator and cryogenic fuel layer in the above equation, the imploded configuration must be spherical to <25%. This degree of sphericity requires a time average x-ray flux uniformity of about 1%. Depending on the time duration, the target can tolerate symmetry variations which are 5-10%. The ignition capsules can also tolerate several hundred picoseconds of variation in the pulse shape timing. The NIF laser specifications have been chosen so that pointing, power balance, and pulse shape specifications are

3

consistent with this degree of precision. For example, pointing errors of 50 μm rms produce a capsule asymmetry <0.3% and power balance errors of 8% rms produce an asymmetry of <0.5%. The expected level of uncertainty from the laser specifications and the tolerable variations are indicated in Table I.

Table I Integrated calculations show that sensitivities of the PT target design are consistent with NIF specifications. Tolerable variations correspond to FWHM in yield, based on integrated calculations. Expected variations are preliminary estimates of system uncertainty, based on NIF laser specifications and experimental uncertainties.

Laser Parameter	Tolerable	Expected
Power during foot	30%	<5%
Peak power	35%	<5%
Second rise timing	500 ps	<100 ps
Third rise timing	500 ps	<100 ps
Duration of peak power	800 ps	<100 ps
Inner beam power during foot (total power fixed)	25%	<5%
Inner beam power during peak (total power fixed)	35%	<5%
Inner beam power during peak (outer cone power fixed)	25%	<5%
Pointing of inner beams	200 μm	<200 μm
Pointing of outer beams	350 μm	<20 μm

Because of computer size constraints, we are not able to include the microphysics of laser/plasma interaction or the short spatial scale hydrodynamic instabilities in these integrated calculations. The laser/plasma coupling is treated as a constraint which limits the achievable hohlraum temperature. The short spatial scale hydrodynamic instabilities are treated in separate calculations which include the effects of asymmetry on the capsule from the integrated calculations.

Hohlraums which achieve 300 eV radiation temperatures in NIF size, geometry, and time scales, produce large volumes of plasma at a density of $\sim 10^{21}/cm^3$ with temperatures of 4-5 keV. The single beam laser intensity at a laser wavelength of 0.35 μm is $1-2 \times 10^{15}$ W/cm² during the peak of the laser pulse. As shown in Fig. 5, extensive experiments on the Nova laser have demonstrated that under these conditions, it will be possible to limit the combined level of SBS and SRS to less than 10% [5]. To achieve these levels, SSD beam smoothing with 2-3 Å of bandwidth will probably be required. Current topics of research include nonlinear saturation mechanisms and coupling between SBS and SRS [6,7].

As indicated in Fig. 2, the NIF hohlraum design utilizes a low-z gas fill. This fill insures that the laser absorption occurs primarily near the hohlraum wall, as required for efficient symmetry control. Early Nova experiments, which showed excellent control of symmetry and good agreement between LASNEX calculations and experiment, did not have this gas fill [1]. Experiments on Nova over the past two years have shown that symmetry can also be controlled in gas-filled hohlraums. As shown in Fig. 6, the implosion symmetry in gas filled hohlraums can be tuned by varying the length of the hohlraum. The sensitivity to changes in hohlraum length is essentially the same as for hohlraums without gas. However, the gas-filled hohlraums show a shift in the hohlraum length for optimum symmetry which is not predicted by LASNEX. This shift is about 150 ± 25 μm, or about 20% of the diameter of the laser spot on the hohlraum wall[8,9]. These results are for hohlraums having 1 atm of methane gas fill which have a plasma density similar to NIF hohlraums. There is an increasing body of evidence that this shift is due to the effects of plasma flow across the laser beam on laser beam filamentation. The Nova laser beams have significant modulation, this modulation leads to filamentation as the beam propagates toward the hohlraum wall. Pondermotive and thermal effects in high intensity portions of the beam act to expel plasma from those regions. Refraction of the beam in the reduced density plasma leads to an enhance intensity and an increased expulsion of plasma. Without flow across the beam, this

4

Total SBS reflectivity

Total SRS reflectivity
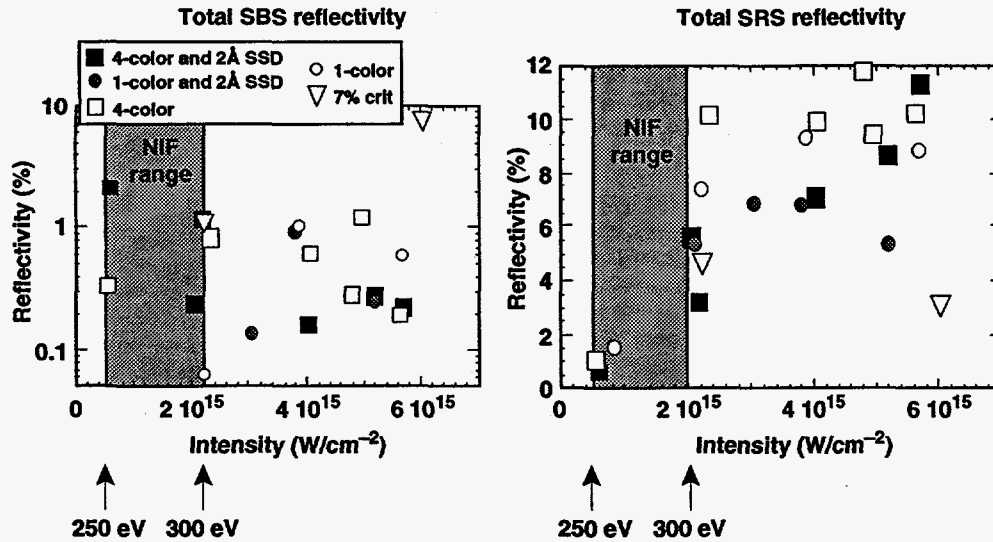
08-00-0595-1186Apb01

Fig. 5   A variety of targets has been used on Nova to simulate NIF-like plasma conditions. Data shown was obtained from submicron thick plastic balloons filled with neopentane at a density $n/n_c \sim 0.1$ where $n_c=9 \times 10^{21}/cm^3$ is the critical density for 0.35 μm laser light
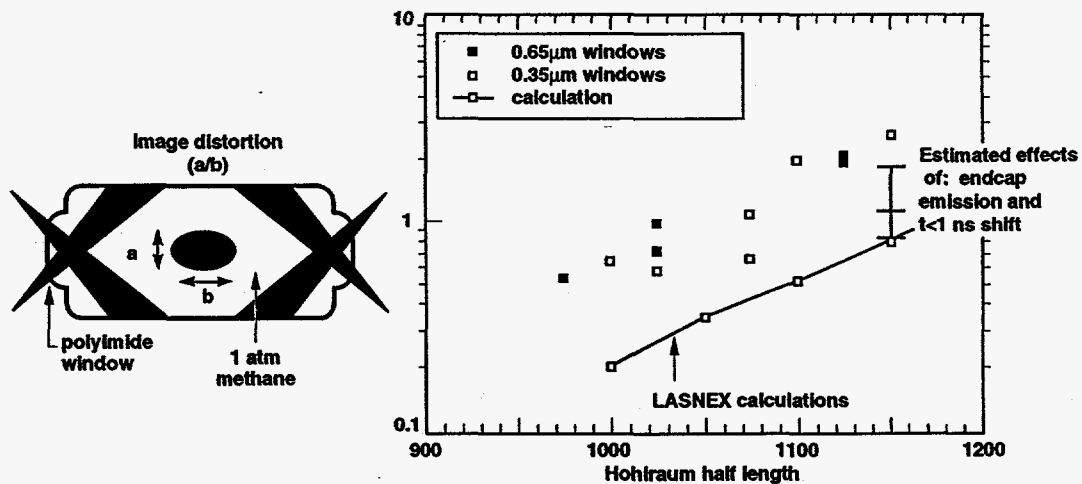
06-00-0996-2105pb01
EJDL/sss

Fig. 6   Symmetry experiments with gas-filled hohlraums show the same sensitivity to beam pointing as earlier vacuum hohlraums. However, there is an offset between the measured and calculated image distortions equivalent to a 150 ± 25μm shift in beam pointing. Emission profiles taken with RPP-smoothed beams indicate that beam smoothing will bring symmetry into agreement with LASNEX modeling.

process is spatially symmetric and the average propagation direction of the beam is unaffected. However, with flow across the beam, the plasma profiles which result from filamentation are asymmetric, resulting in a deflection in the beam propagation direction [10,11]. This process, which is not included in LASNEX, is expected to produce an angular deflection in NIF targets which is comparable to that in Nova targets [11]. Compared to targets without a gas fill, Nova experiments show a shift in the x-ray emission pattern which is sufficient to account for the symmetry shift [9]. In experiments which utilized a slot in the hohlraum wall, this shift is composed of an early time shift in the laser spot location, and a late time redistribution of energy toward the laser entrance hole which is consistent with filamentation in flow. Use of SSD beam

5

smoothing is calculated to greatly reduce the effects of filamentation on Nova and NIF beams. Experiments on Nova have shown that even a Random Phase Plate (RPP) alone, without bandwidth, can largely eliminate the shift in the x-ray emission pattern seen in gas filled hohlraums. To date, these experiments have been carried out with only a single beam on Nova. Symmetry experiments with SSD on all 10 Nova beams are being planned.

All ignition target designs require that the bulk of the fuel be in a cryogenic layer on the inside surface of the ablator. Bulk heating of the DT by β-decay of the tritium provides an effective technique for producing uniform layers of DT in ICF targets. If the capsule outer surface is at a uniform temperature, β-decay will cause thick regions of DT be at a higher temperature than thinner regions. These hotter regions will sublime more rapidly and become thinner. This process continues until the layer has a nominally uniform thickness. However, the DT tends to deposit as a large number of small crystallites. The β-heating process does not completely eliminate discontinuities which arise at the boundaries of these crystallites, resulting in about a 1 μm micro-scale roughness[12]. The β-decay in 50/50 DT produces about 0.16 watt per gram. If external heating is applied to augment the β-decay, smoother layers can be produced. Both optical techniques, which couple to rotational/vibrational transitions in DT, and radio frequency heating, which couples to the free electrons produced by β-decay, have been shown to produce smoother DT layers [13]. The optical absorption technique applies equally well to DD or DT fuel. This will be important in non-ignition experiments which may utilize DD fuel.

The effects of Rayleigh-Taylor instabilities are modeled in a variety of ways. The NIF ignition targets are designed to remain in the linear or weakly nonlinear regime. Because of this, it is possible to develop a model of the effects of hydrodynamic instability which is based on linear analysis, with an extension into the weakly nonlinear regime [14,1]. The most thoroughly tested approach utilizes a series of 2-D single mode LASNEX calculations which are run in the small amplitude linear regime to develop a dispersion relation. It is easy to check linearity, mode preservation, zoning convergence, and other numerical issues in these calculations. Such single mode calculations are also close to a large Nova data base which is modeled the same way. These growth factors are combined with an assumed initial surface spectrum to determine the ignition time perturbation layer thickness. In this approach, the effects of this perturbed layer on the ignition hot spot are evaluated using a one-dimensional model in which thermal mixing is represented as an enhanced thermal conductivity in the perturbed region.

To test the weakly nonlinear analysis, full simulations of multimode perturbations with realistic initial amplitudes are also run, although the number of modes that can be included is limited. A variety of two-dimensional multimode simulations have been run on several capsules, at solid angles ranging from relatively small conic sections to half spheres. Results are consistent with the weakly nonlinear analysis above but this is an area of current work [3,4].

The growth of perturbations in the linear regime, for perturbations with the same wavenumber, is the same in 2-D and 3-D. However, simulations of the Rayleigh-Taylor (RT) instability on classical interfaces [15-19], as well as on foils driven by laser light [20,21] and x-rays[22] predict that symmetric three-dimensional perturbations should grow largest in the nonlinear regime. These predictions, along with those of third order perturbation theory,[23] are consistent with results of single mode RT experiments done on an air-water interface[24] and on foils driven by x-rays.[22] . Because of the dependence of nonlinear saturation amplitude upon perturbation shape, direct 3-D simulations represent the most accurate method of modeling the nonlinear evolution of hydrodynamic instabilities which evolve from realistic surface perturbations.

Development of the three-dimensional HYDRA code has allowed us to perform the first 3-D multimode simulations of the PT ignition capsule design. HYDRA[25], is a 3-D radiation hydrodynamics code with arbitrary Lagrange Eulerian (ALE) capability. For simulations of ignition capsules HYDRA uses a thermonuclear burn package to treat the depletion and production of isotopes. An efficient multigroup routine transports energetic charged particles produced during the burn phase. Since the capsules are thin to neutrons, an accurate treatment of neutron energy deposition is obtained with a neutron transport model derived in the free streaming limit. As energetic particles slow down, they deposit energy in separate electron and ion channels. Electron and ion conduction are treated, as well as electron-ion energy exchange.

Hydrodynamic instabilities were simulated over a portion of the capsule solid angle which extends equal amounts in the polar and azimuthal angles $(\Delta\theta, \Delta\phi)$, with one boundary coincident with the capsule equator. Multimode surface perturbations imposed were of the form $G(\theta, \phi) = \Sigma_m \Sigma_n a_{mn} \cos(m\pi\theta/\Delta\theta) \cos(n\pi\phi/\Delta\phi)$, with symmetry boundary conditions at transverse boundaries. These are analogous to modes used in previous 2-D axisymmetric simulations over a portion of a quadrant [3]. Perturbations on the outer ablator surface are based upon traces from a Nova capsule, while those on the inner DT surface are based upon measurements of cryogenic ice.

6

This information is converted to an estimated 3-D power spectrum [26], and power is distributed isotropically among the 3-D modes with equivalent wave number.

As an example we consider a capsule having perturbation amplitudes, in the range of modes $l \geq 10$, equal to 24 nm rms on the outer surface and 1 μm on the inner cryogenic DT surface. Modes in the range $l=10\text{-}40$ are simulated over a domain extending 18 degrees in each angle. These are the modes most capable of generating spikes of cold fuel during the compression of the hot spot. During the implosion phase, the simulated shell areal density strongly resembles the initial outer surface perturbation. This demonstrates that the modes which grow in the ablator are seeded predominantly by initial ablator surface perturbations, not from the perturbed rarefaction wave which returns from the ice surface after the first shock breaks out. Depressions initially on the surface develop into bubbles in the ablator surrounded by interconnecting spike sheets and larger individual spikes.

Figure 7 shows bubble and spike ridge structures which are growing on the pusher-hot spot interface after the rebounding shock has reached it. These correspond to the locations of the equivalent lower mode structures in the ablator which have fed through the shell. The resemblance to the initial surface perturbation is characteristic of weakly nonlinear behavior. Only very late in the simulation, as the capsule approaches ignition, does the perturbation structure on the inner surface evolve toward lower mode numbers. This behavior appears to be strongly influenced by conductive ablation and the effect of convergence in this case, rather than by mode coupling, as was seen in planar geometry [21,27,28,29].

Figure 8 shows yields from simulations of several PT capsules having different multimode surface perturbations containing modes in the range $l=10\text{-}40$. The capsule having the largest perturbation amplitudes failed to ignite because at the time of stagnation spikes had penetrated 10 μm into the 30 μm radius hot spot. The location of the yield cliff corresponds to a roughness on the outer surface which is ~40% smaller than obtained with previous 2-D multimode simulations over this range of modes. Results from a 3-D multimode simulation have been compared with an axisymmetric 2-D HYDRA simulation having equivalent initial rms surface roughness. The comparison confirms that the higher nonlinear growth rates which are obtained for the round 3-D bubble-spike features than for the 2-D bubble-spike ridges are responsible for the smaller allowable surface roughness found in these calculations.
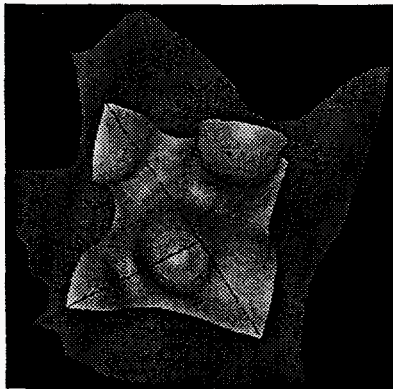

Fig 7 Iso-density contour surfaces of 60 g/cm³ near ignition time from a PT capsule simulation having 24 nm and 1 μm rms perturbations initially on the outer ablator and inner ice surfaces respectively. The perspective shows the pusher-hot spot interface viewed from the inside.
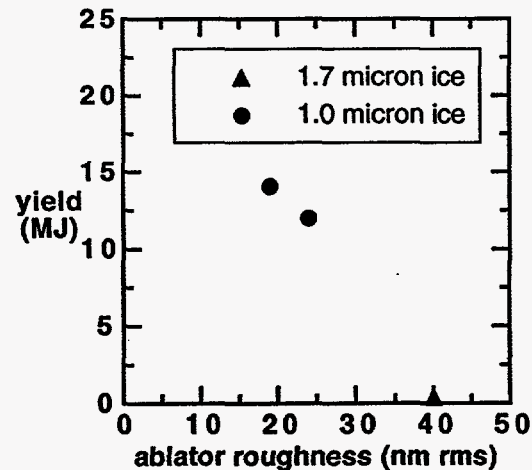
Fig. 8 Yields from HYDRA PT capsule simulations performed with various roughness on the ablator and cryogenic ice. Perturbations initialized contained modes with l=10-40.

RT unstable modes in the range $40 < l < 120$ are much less capable of feeding through the shell and producing spikes upon deceleration than the modes considered above. But they can threaten the shell integrity during the implosion phase, when the shell is thinnest. We have simulated surface perturbations which include modes spanning both of these ranges ($l = 15\text{-}120$)

on a 12 degree wedge. The outer surface corresponded to the best surface finish measured on a Nova capsule. The surfaces simulated have amplitudes of 21 nm and 1.3 μm peak-to-valley on the outer ablator and inner DT ice respectively. The simulation shows the shell integrity is well preserved throughout the implosion. Figure 9a,b shows the iso-density contours corresponding to locations just inside the DT-ablator interface and at the pusher-hot spot interface close to ignition time. The high modes apparent in Fig. 9a, typically in the range l=90, have not fed through appreciably to the inner interface, which has features typically in the range l=15-20. The yield, 15.5 MJ, approaches the value obtained for an unperturbed capsule. Thus a PT capsule with a surface finish equal to the best measured on a Nova capsule easily ignites in the simulation. The margin of ignition in this simulation implies that substantially larger perturbation amplitudes can be tolerated on the outer surface than were used in this case, even with high-l modes present. Future work will quantify the sensitivity of the capsule to surface roughness contained in different ranges of modes.
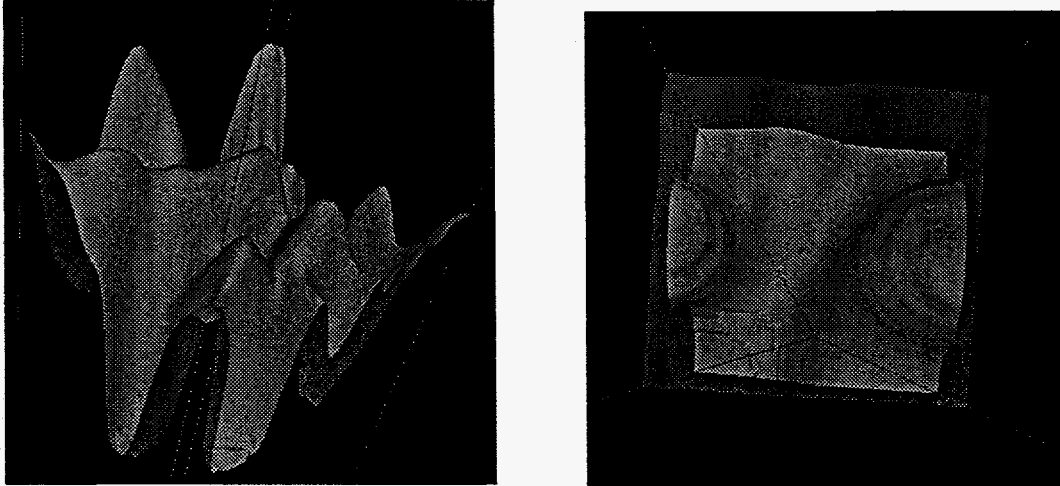

Fig. 9   Iso-density contour surfaces near ignition time for a PT capsule simulation containing modes with l=15-120. (a) 130 g/cm³ surface just inside the DT-ablator interface (b) 650 g/cm³ surface at pusher-hot spot interface seen from the inside.

Single mode radiation driven planar experiments mentioned earlier [22] demonstrated the effect of mode shape on perturbation growth and provided a test of the ability of HYDRA to simulate accurately these efforts.

Also, capsules with multimode surface perturbations, created by ablating pits with a laser at 200 randomly selected locations, have been used in Nova experiments to quantify the degradation of implosions subject to near NIF levels of hydrodynamic instability. HYDRA simulated multimode growth on these capsules over a 1/20 sphere domain, extending from the pole to the equator and 36 degrees in azimuthal angle, with symmetry conditions at transverse boundaries. The perturbation simulated was based upon a portion of the actual surface, projected onto spherical harmonics compatible with the boundary conditions. Figure 10 shows a portion of the classical fuel-pusher interface at 2.05 ns, near bang time, for a Nova capsule having an initial 0.15 μm rms multimode surface perturbation. The bubbles are rising at the same locations initially occupied by pits ablated on the outer surface. Modal analysis of the shell perturbation structure indicates that most of the spectrum is due to growth of modes initially present, an indication of weakly nonlinear behavior.

Other sources of asymmetry, besides those imposed on the capsule surface, are found to be important in the simulations of Nova capsules. The relatively small number of beams on Nova leads to substantial 3-D azimuthal variation in the hohlraum x-ray drive. The variation in radiation drive is large enough in the Nova hohlraum that 3-D coupling with imposed surface perturbations can have a dramatic effect on simulated capsule performance. Low mode drive asymmetry combined with surface roughness can cause a few spikes to approach the capsule center ahead of the rest. These can continue into the capsule center nearly in free fall. Figure 11 compares experimental yields for Nova capsules having multimode surface perturbations with yields from HYDRA simulations and from our 1-D mix model[30]. For the rough 1 μm rms capsules there is good agreement between the 1-D model and experimental yields. But the experimental yields for
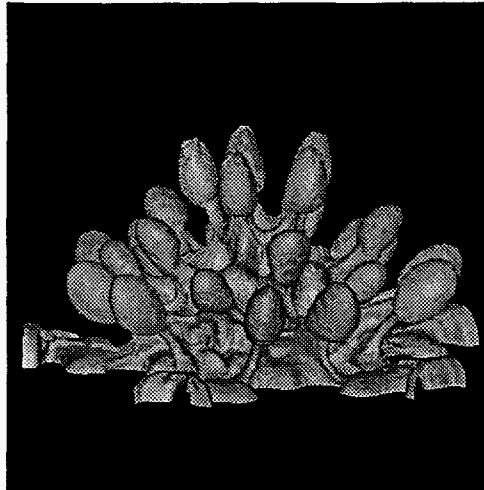
Fig. 10 A hemispherical portion of the fuel-pusher interface seen from the outside near bang time for a Nova capsule having an initial 0.15 μm multimode perturbation.

smoother capsules are substantially less than the 1-D model predicts. The 3-D HYDRA simulations which include imposed surface roughness and radiation drive asymmetry, shown as squares in Fig. 11, give lower yields for the smoother capsules which are closer to the data. Low mode wall thickness variations are also present in these Nova capsules. HYDRA simulations which also include low mode thickness variations having peak-to-valley amplitudes typical of measured values, oriented to enhance the effect of coupling, are shown as triangles in Fig. 11. Coupling between the various asymmetries results in spikes quenching the hot spot prior to bang time. When the combined effects of known asymmetries are included, the 3-D simulations produce neutron yields which are close to the experimental values. The effect of pointing errors and power imbalance will be examined in future simulations.
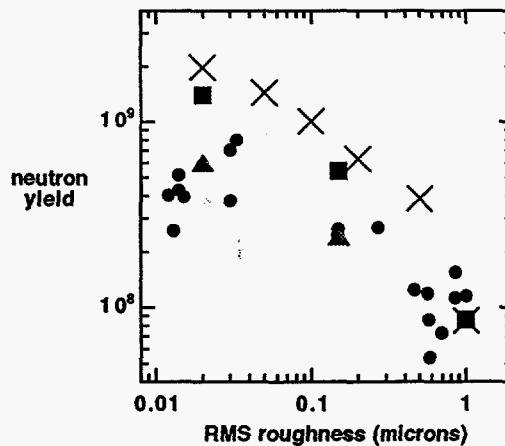

Fig. 11 Solid circles show experimental yields of Nova capsules having multimode perturbations of various amplitudes. The crosses indicate yields from the 1-D mix model. The solid squares are from 3-D HYDRA simulations, including drive asymmetry. The triangles represent simulations which also include low mode thickness variations.

The advances in NIF target design together with the advances on Nova on laser/plasma coupling, symmetry in gas-filled hohlraums, hydrodynamic instability, and cryogenic layer uniformity have resulted in a recommendation by the ICFAC, the U.S. Department of Energy (DOE) advisory board on ICF, that DOE move ahead with detailed engineering design of the NIF.

REFERENCES

[1]   LINDL, J.D., Phys. Plasmas 2(11), 3933 (1995).
[2]   ZIMMERMAN, G.B. and KRUER, W.L., Comm Plasma Phys 2,51 (1975).
[3]   HAAN, S.W., et al., Phys. Plasmas **2**, 2480 (1995).
[4]   KRAUSER, W.J., HOFFMAN, N.M., WILSON, D.C., WILDE, B.H., VARNUM, W.S.,
        HARRIS, D.B., SWENSON, F.J., BRADLEY, P.A., HAAN, S.W., POLLAINE, S.M.,
        WAN, A.S., MORENO, J.C., and AMENDT, P.A., Phys. Plasmas **3**, 2084 (1996).
[5]   McGOWAN, B.J., et al., Phys. Plasmas 3(5), 2029 (May 1996).
[6]   KIRKWOOD, R.K,. et al. to be published Phys. Rev. Lett. Sept 9 (1996).
[7]   FERNANDEZ, J.C., et al. to be published Phys. Rev. Lett. Sept. 9 (1996).
[8]   DELAMETER, N.D., et al., Phys. Plasmas 3,2022 (1996).
[9]   POWERS, L.V., et al. , Proceedings of the 24th European Conference on the Interaction of
        Lasers with Matter, Institute of Physics Publishing, London, 1996 (to be published).
[10]   ROSE, H.A., Phys. Plasmas 3(5),1709 (May 1996).
[11]   HINKEL, D.E., WILLIAMS, E.A. and STILL, C.H., Phys. Rev. Lett. 77,1298 (1996).
[12]   SANCHEZ, J., Lawrence Livermore National Laboratory and HOFFER, J., Los Alamos
        National Laboratory, personal communication (1995).
[13]   COLLINS, G., et al., "Heat-flux induced changes to multicrystalline d2 surfaces," LLNL
        report UCRL-JC-124261 (1996).
[14]   HAAN, S., Phys, Rev. A 39,5812 (1989)
[15]   TRYGGVASON, G., and UNVERDI, S.O., Phys. Fluids A **2**, 656 (1991) .
[16]   YABE, T., HOSHINO, H., and TSUCHIVA, T., Phys. Rev. A **44**, 2756 (1991).
[17]   HECHT, J., OFER D., ALON, U., SHVARTS, D., ORSZAG, S.A., and McCRORY, R.L.,
        Laser Part. Beams 13, 423 (1995); OFER, D., HECHT, J, SHVARTS, D., ZINAMON, Z.,
        ORSZAG, S. A., and McCRORY, R. L., *Proceedings of the 4th International Workshop
        on the Physics of Compressible Turbulent Mixing,* edited by LINDEN, P. F., YOUNGS, D.
        L., and DALZIEL, S. B. (Cambridge University Press, Cambridge, 1993), p. 199.
[18]   SAKAGAMI, H. and NISHIHARA, K., Phys. Rev. Lett. **65**, 432 (1990).
[19]   TOWN, R.P.J. and BELL, A.R., Phys. Rev. Lett. **67**, 1863 (1991).
[20]   DAHLBURG, J.P., GARDNER, J.H., DOOLEN, G.D., and HAAN, S.W., Phys. Fluids B
        5, 571 (1993).
[21]   DAHLBURG, J.P., FYFE, D.E., GARDNER, J.H., HAAN, S.W., BODNER, S.E., and
        DOOLEN, G.D., Phys. Plasmas **2**, 2453 (1995).
[22]   MARINAK, M.M., REMINGTON, B. A., WEBER, S. V., TIPTON, R. E., HAAN, S.W.,
        BUDIL, K.S., LANDEN, O.L., KILKENNY, J.D., and WALLACE, R., Phys. Rev. Lett.
        75, 3677 (1995).
[23]   JACOBS, J. W. and CATTON, I., J. Fluid Mech. **187**, 329 (1988).
[24]   JACOBS, J.W. and CATTON, I., J. Fluid Mech. **187**, 353 (1988).
[25]   MARINAK, M.M., TIPTON, R.E., LANDEN, O.L., MURPHY, T.J., AMENDT, P.,
        HAAN, S.W., HATCHETT, S.P., KEANE, C.J., McEACHERN, R., and WALLACE, R.,
        Phys. Plasmas **3**, 2070 (1996).
[26]   See National Technical Information Service Document No. DE 95-011970 (POLLAINE,
        S.M., HATCHETT, S.P., and LANGER, S.H., "Spectral analysis of ICF capsule surfaces,"
        ICF Quarterly Report, Vol. 4 (3), p. 87, UCRL LR-105821-94-3). Copies may be ordered
        from the National Technical Information Service, Springfield, Virginia 22161.
[27]   SHARP, D. H., Physica D **12**, 3 (1984).
[28]   ALON, U., SHVARTS, D., and MUKAMEL, D., Phys. Rev. E **48**, 1008 (1993); Phys.
        Rev. Lett. **72**, 2867 (1994).
[29]   SHVARTS, D., ALON, U., OFER, D., McCRORY, R.L., and VERDON. C.P., Phys.
        Plasmas **2**, 2465 (1995).
[30]   KEANE, C.J., POLLAK, G.W., COOK, R.C., DITTRICH, T.R., HAMMEL, B.A.,
        LANDEN, O.L., LANGER, S.H., LEVEDAHL, W.K., MUNRO, D.H., SCOTT, H.A., and
        ZIMMERMAN, G.B. , J. Quant. Spectrosc. Radiat. Transfer **54**, 207 (1995).